

Common Envelope Evolution

Ronald E. Taam,^a Paul M. Ricker^b

^a*Department of Physics and Astronomy, Northwestern University, Evanston, IL 60208*

^b*Department of Astronomy, University of Illinois, Urbana, IL 61801*

Abstract

The common envelope phase of binary star evolution plays a central role in many evolutionary pathways leading to the formation of compact objects in short period systems. Using three dimensional hydrodynamical computations, we review the major features of this evolutionary phase, focusing on the conditions that lead to the successful ejection of the envelope and, hence, survival of the system as a post common envelope binary. Future hydrodynamical calculations at high spatial resolution are required to delineate the regime in parameter space for which systems survive as compact binary systems from those for which the two components of the system merge into a single rapidly rotating star. Recent algorithmic developments will facilitate the attainment of this goal.

Key words: binaries: close – hydrodynamics

1 Introduction

The evolutionary study of close binary systems with compact neutron star and black hole components has been a major focus of stellar X-ray astronomy ever since the seminal contributions by van den Heuvel and Heise (1). Since then, the discovery of compact stars in interacting binary systems has had an enormous impact on our basic understanding of the properties of these stars, on the manner in which mass is transferred from a stellar donor to its compact accretor, and on the evolution of these

systems (2; 3). The recent *Chandra* and *XMM-Newton* observations of the point X-ray source population in the Milky Way and in external galaxies have led to a renewed interest in studying the evolution of these compact systems in a variety of galactic environments.

Among the trademarks of the evolutionary scenarios presented in van den Heuvel and Heise (1) are the cartoons used to depict the evolution of binary systems to the compact stage. These have now become the standard means of visualizing the possible evolutionary channels. For

a recent review of the formation and evolution of compact X-ray sources, see Tauris & van den Heuvel (3). Central to the construction of these channels is the existence of a common envelope or spiral in phase in which significant mass and orbital angular momentum are lost from the system. In this phase, the system is transformed from one of long orbital period to one of short orbital period (4). One of the members of the system, a star with an evolved core in the red giant or asymptotic giant branch star, expands beyond the orbit of its companion. Provided that the stellar components are not in state of synchronous rotation at the onset of mass transfer, the asynchronous interaction of the two components can lead to the conversion of orbital energy into the kinetic energy of outflow of the common envelope. As a result, it was envisioned that a main sequence-like companion spirals toward the core of the giant. The common envelope is ejected leaving behind the progenitor remnant of the compact component with its companion at separations which are significantly smaller than the original radius of the giant progenitor (see reviews by Iben & Livio (5) for evolutions involving intermediate mass stars and Taam & Sandquist (6) for evolutions involving massive stars). Among the classes of binary systems for which the common envelope phase plays an important role are systems with neutron star (binary radio pulsars, X-ray binaries), black hole (X-ray sources), or white dwarf (cataclysmic variables) compact components.

In the next section, the evolution leading to the common envelope phase is described without reference to the evolution resulting from the collisional interactions in dense stellar systems (7; 8; 9). Of particular importance, here, are the conditions leading to the establishment of a non-corotating common envelope in primordial binary systems. The various stages of the ensuing spiral in phase are presented in section 3, and the conditions leading to the successful ejection of the common envelope are described in section 4. Finally, we provide an overview of the results from hydrodynamical simulations and discuss the prospects of high spatial resolution calculations in the near future in the last section.

2 Evolution to the common envelope stage

The binary system can enter into the common envelope stage when its total systemic angular momentum is less than its minimum value for components in synchronous motion. In this case, it evolves away from synchronism as a result of a tidal instability (10; 11; 12; 13; 14). This critical limit for synchronous systems exists because the spin angular momentum of the more evolved and significantly larger stellar component can become comparable to the orbital angular momentum of the system. A synchronously rotating star which evolves to this point cannot evolve to ever larger radii and still remain synchronized to the or-

bital motion. Instead, the two components of the system are driven out of synchronism by the action of tidal forces and viscous dissipation, shrinking the orbit as orbital angular momentum is converted into spin angular momentum of the larger component of the system. For a star of a given radius, the spin angular momentum ($J_{spin} \propto a^{-3/2}$) increases with decreasing orbital separation, a , while the orbital angular momentum decreases ($J_{orb} \propto a^{1/2}$). Hence, for sufficiently small orbital separations, the rotational angular velocity of the more evolved stellar component cannot be maintained at the orbital angular velocity of its companion. This evolution leading to a spiral in phase takes place for binary systems characterized by large mass ratios. For example, systems with a red giant or asymptotic giant branch component would undergo this tidal instability for mass ratios greater than about 5-6.

An alternative path to the common envelope stage can occur whenever the rate of mass transfer is sufficiently high such that the timescale for angular momentum redistribution between the spin and the orbit required to bring the components of the system into a state of synchronous rotation is longer than the mass transfer timescale. This evolutionary channel can take place when the mass transfer rate accelerates due to an imbalance between the variation of the stellar radius and the star's corresponding Roche lobe with respect to mass loss. This mass transfer instability is particularly relevant to systems in which the more massive

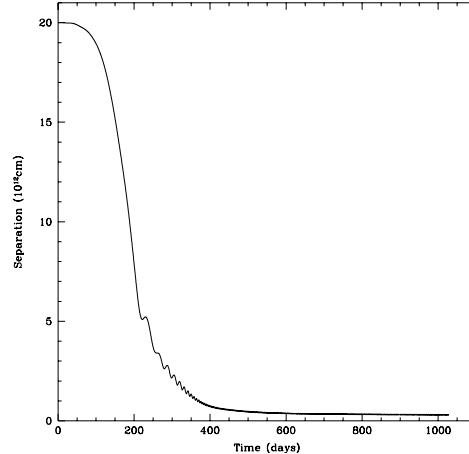


Fig. 1. The orbital separation as a function of time for a system composed of an asymptotic giant branch star of $3M_{\odot}$ with a core mass of $0.7M_{\odot}$ synchronously rotating with a $0.4M_{\odot}$ main sequence companion for a system with an initial orbital period of 0.84 yr (28).

star is characterized by a deep convective envelope. In this case, there is a tendency for the donor to expand while its corresponding Roche radius decreases as mass is lost. The accretor is also likely to expand since it accretes at a rate faster than its thermal timescale and cannot assimilate the accreted mass in a state of thermal equilibrium. As a result, both components are expected to fill or exceed their respective Roche lobes. In this pathway, systems in which the more massive star undergoes mass transfer while in the Hertzsprung gap or in the red giant or asymptotic branch phase can enter the common envelope phase either via a direct or a delayed dynamical instability (15). We note that evolution to the common envelope stage via a mass transfer instability is not limited to accreting non degenerate stars, but can also apply to compact accreting neutron stars (16) as well.

3 Evolutionary stages

Substantial progress in the description of the spiral in evolution has been achieved from investigations of increasing complexity and realism. Building on the early studies in both one (17; 18; 19) and two (20; 21; 22; 23) dimensional modeling, the studies based on three dimensions (24; 27; 25; 26; 28; 29) have provided significant understanding of the conditions leading to successful ejection of the common envelope. A particularly challenging aspect of the multi-dimensional calculations is the wide range of timescales and length scales that must be modelled. In particular, the timescales range from hours during the late stages to years at the onset of the common envelope phase, and the length scales range from Earth-like dimensions to more than an astronomical unit. As a result, the hydrodynamical calculations that have been reported are primarily exploratory in nature. On the other hand, the existing computations have provided insight into the essential features introduced by the additional dimensionality considered in the problem and the important physical processes required for a detailed description underlying our understanding of this evolutionary channel. In the following, we provide an overview of the several distinct stages of the common envelope phase, focusing on the evolution during the deep spiral in phase to short orbital periods and the terminal phase leading to the formation of the final post common envelope system. To these individual phases

we now turn.

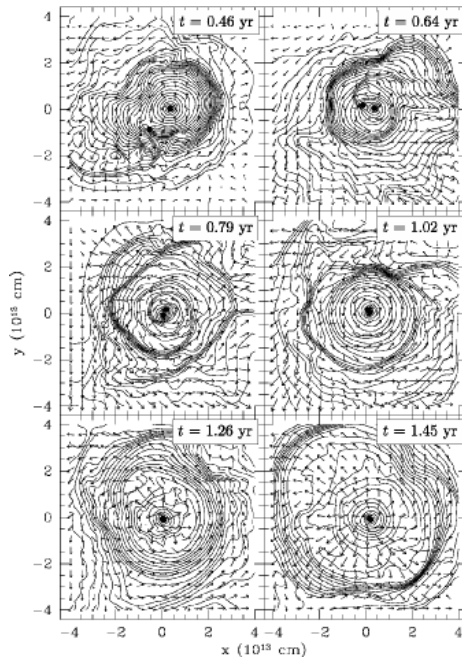


Fig. 2. The density distributions and velocity fields in the orbital plane of the binary described in Figure 1 (28). The density contours are logarithmic and are spaced five per decade. The velocity vectors are scaled to the maximum in each panel. The solid dots indicate the position of the cores and the distributions are at times given in each panel. Spin up can be seen at a time of 1.02 yrs with material outflow subsequently taking place (e.g., see panels at times 1.26 and 1.45 yrs).

3.1 Deep spiral in

To illustrate a typical binary system, in the common envelope phase, in Figure 1 we show the orbital separation as a function of time for an asymptotic giant branch star with a low mass main sequence companion. It is clearly evident that the separation between the two cores

decreases rapidly (on a timescale of about 100 days). During the inspiral, the outer layers of the common envelope are tidally stripped in the orbital plane, leading to the formation of an outflowing circumbinary disk of material. The relative orbit of the two cores becomes very eccentric during the early phase of evolution as most of the orbital angular momentum is converted to spin angular momentum in the outer envelope layers. However, as the two cores spiral closer together, a greater fraction of orbital energy is lost at smaller separations in comparison to orbital angular momentum, causing the orbit to become more circular.

The rapid orbital decay of the system causes envelope material to accelerate relative to the companion star, leading to the formation of shocks in the envelope. As the system evolves to ever smaller orbital separations, the shocks evolve into a tighter and tighter spiral structure pattern. The interaction of the shocks with the envelope converts the orbital angular momentum of the two stellar components into the spin angular momentum of the common envelope. As a result, matter in the common envelope is spun up to nearly circular motion (see figure 2). This spin up effectively causes an outward force, as centrifugal effects help to expand material to greater distances from the two cores. As shown in Figure 3, common envelopes involving massive supergiant stars also show this behavior (6).

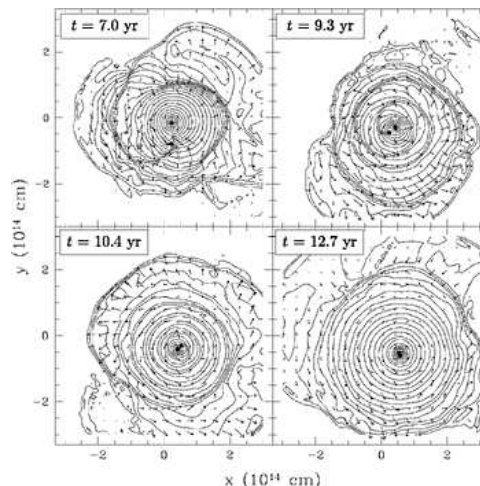


Fig. 3. The density distributions and velocity fields in the orbital plane of a binary composed of a $20M_{\odot}$ red supergiant with a $1.4 M_{\odot}$ companion at different evolution times(6). Density contour levels correspond to 5 per decade, and the velocity field is scaled to 60 km s^{-1} in all panels. The evolutionary state of the massive star is at the onset of core carbon burning. A tightly wound spiral emerges as the orbital velocities of the two cores exceed the rotational velocity of the envelope gas. The solid dots indicate the position of the cores and the initial orbital period is 10.6 yr. Spin up occurs at time 10.4 yr, leading to an outward flow at a time of 12.7 yr.

3.2 Final stage

Since the orbital energy is deposited into the common envelope on a dynamical timescale in the orbital plane, the ejected material is concentrated toward this plane. The ejection, however, is nearly axisymmetric with respect to the angular momentum axis since the timescale on which the energy is deposited (comparable to the local orbital period) is less than the timescale of orbital decay in this stage. The flow is not

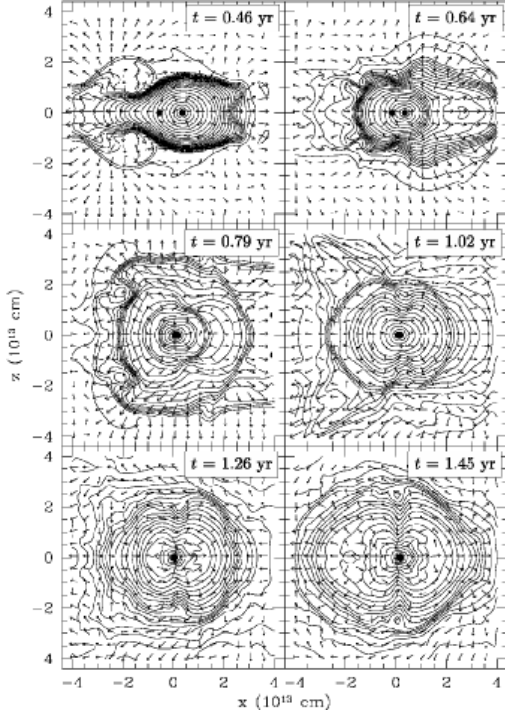


Fig. 4. The density distributions and velocity fields in the plane perpendicular to the orbital plane at the times for the system in Figure 2 (28). Density contours and velocity vectors are as in Figure 2.

purely radial, as can be seen most clearly at a time of 1.45 yr in Figure 4, where a circulatory flow between the equatorial plane and the polar direction results.

Spin up to a greater degree is found for a red giant progenitor with a low moment of inertia either due to low envelope mass or relatively small radius. In this case, a greater density contrast between the polar and equatorial directions can develop. This may be relevant to the bi-polar morphology of a class of planetary nebulae. Figure 5 illustrates the density and velocity distribution in the plane perpendicular to the orbital plane for two systems in which the

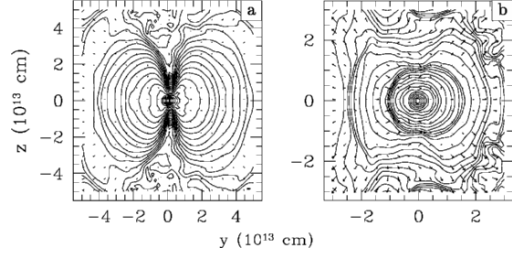


Fig. 5. The density contours and velocity field in the plane perpendicular to the orbital plane after the rapid infall phase (29). Density contours are 5 per decade, and the velocity fields in each panel are scaled to a maximum speed of 60 km s^{-1} . The mass of the red giant core and companion in the common envelope binary are $0.45M_{\odot}$ and $0.35M_{\odot}$, respectively. The mass of the red giant in panel (a) is $1M_{\odot}$, and in panel (b), $2M_{\odot}$. Note that a sharper density contrast between equatorial and polar directions results in the case for which the mass of the companion is comparable to the mass in the common envelope.

mass of the companion and the mass of the red giant core are $0.35M_{\odot}$ and $0.45M_{\odot}$ respectively. The structure in panel (a) for a $1M_{\odot}$ red giant and in panel (b) for a $2M_{\odot}$ red giant illustrates the dramatic difference in the common envelope structure when the degree of spin up is great. Note the evacuation of matter along the polar directions. Eventually an outflow is produced that is concentrated in the equatorial plane.

The evolution enters the terminal phase as the companion further spirals into the common envelope. The orbital decay rate decelerates because most of the common envelope material has moved to larger radii, where its interaction with the two cores is greatly diminished. As a result, the orbital decay timescale

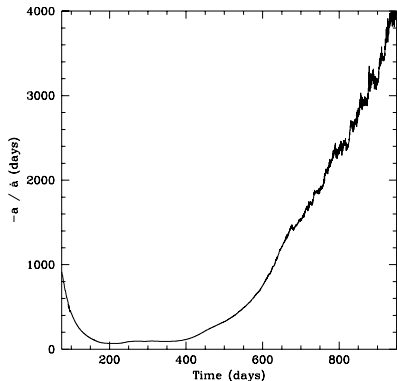


Fig. 6. The orbital decay timescale as a function of time corresponding to the temporal variation of the orbital separation in Figure 1 (28).

dramatically increases from about 100 days to more than 10 years (see Figure 6).

At this point we expect that the material interior to the orbit will contract on its local thermal timescale to the degenerate core of the giant. Although this phase has not been followed, a post spiral in system should be formed with the companion star in close proximity to the remnant core of the former giant.

4 Conditions for successful ejection of the common envelope

The hydrodynamical simulations demonstrate that material in the common envelope is ejected at velocities greater than that required for escape. Although the calculations have not been evolved to the phase in which the entire envelope is lost before the two cores merge, the results to date do provide insight into the conditions necessary for success-

ful ejection of the common envelope to take place.

The primary requirement for ejection of the common envelope is based on energetics. Namely, the energy released from the orbit must exceed the binding energy of the common envelope from *both* stellar components of the system. Generally, the efficiency of mass ejection, as measured by the ratio of the binding energy to the energy lost from the orbit, is less than unity.

Secondly, the rate at which energy is lost from the orbit must be sufficiently high that it can be directly converted into the energy of the outflow rather than being transported to the common envelope surface, where it can be radiated away. For the dynamical evolution described above, the ejection process is rapid and, hence, adiabatic. However the efficiency of mass ejection is less than unity since the mass in the common envelope is preferentially ejected in the orbital plane of the binary system at velocities which are greater than the escape speed.

Finally, the timescale on which the mass is lost from the system must be shorter than the inspiral timescale of the binary, for otherwise the two cores will spiral together and merge before the entire common envelope is ejected.

This latter condition points to the importance of a core envelope structure characteristic of evolved stars on the giant branch. For such stars, the density profile above the nuclear

burning shells is steep so that the mass enclosed in an extensive region is small. Examples of this particular structure are illustrated in Figure 7 for a $20M_{\odot}$ star in different stages of core helium burning and in Figure 8 for a $1M_{\odot}$ red giant star characterized by a range of degenerate helium core masses.

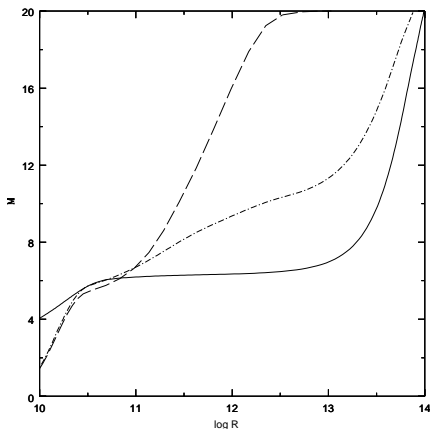


Fig. 7. The variation of mass (in M_{\odot}) with radius for a $20M_{\odot}$ red supergiant. The dashed, dashed dot, and solid curves correspond to a central helium content of 0.5, 0.34, and 0 respectively (6). Note the extensive region between 5×10^{10} and 5×10^{12} cm in which the mass varies very gradually with radius at the stage of carbon core burning.

In both figures an extensive region containing little mass is present. The flat mass profile naturally develops in the late core helium burning stage of a massive star when the central helium content nearly vanishes. For more advanced evolutionary states, the size of this region increases. Similarly, red giant stars show such profiles for helium degenerate core masses greater than about $0.2M_{\odot}$, extending beyond a solar radius for helium core masses greater than about $0.27M_{\odot}$.

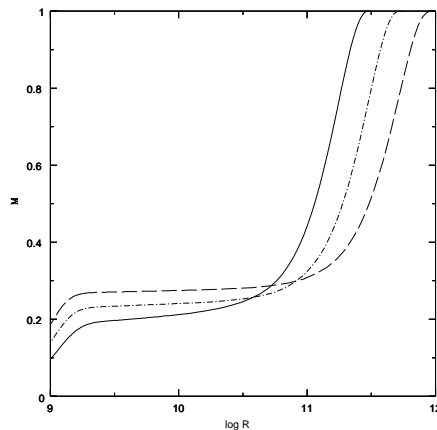


Fig. 8. The mass profile for a $1M_{\odot}$ red giant star in different phases of evolution (29). The solid, dashed-dot, and dashed curves denote evolutionary phases in which the mass of the degenerate helium core is 0.19, 0.23, and $0.27 M_{\odot}$ respectively.

In cases for which the loss of orbital energy does not lead directly to hydrodynamical ejection of the deep layers of the common envelope, mass can still be lost, but on a timescale significantly greater than the dynamical timescale. Here, the rate of energy loss from the orbit supplements the stellar luminosity generated by the nuclear burning shells, enhancing the rate of mass loss via the radiative processes responsible for stellar winds. Such a circumstance may lead to the ejection of the common envelope, especially when the envelope is sufficiently spun up. Detailed calculations reveal that such conditions occur when the mass of the common envelope is comparable to the mass of the inspiraling component. This outcome for the common envelope phase may be related to an alternative prescription for common envelope evolution based on angular momentum arguments under the

implicit assumption that energy is conserved. (30).

Independent of whether the final phase of the common envelope is described as a dynamical or more gradual event, the successful ejection of the envelope requires progenitor stars in the red giant or asymptotic giant phase. For progenitors on the main sequence or in the Hertzsprung gap, it is likely that the binary components will merge in the process, leaving behind a single rapidly rotating star, with possibly a circumstellar disk. The class of rapidly rotating FK Comae giants (31) may be an observational manifestation of such a merger event.

5 Summary and future work

Computational hydrodynamical investigations of the common envelope phase have led to a number of results with significant bearing on the outcome of the post spiral in state of the binary system.

5.1 Overview of results

- The binary orbit decays rapidly after the onset of the common envelope phase, occurring on a dynamical timescale (i.e., on a timescale comparable to the orbital period for which the system entered the common envelope phase).
- As a result of the effectiveness of the gravitational torques in removing orbital angular momentum from the system, the orbit of the

binary system becomes eccentric. Circularization of the binary orbit takes place in the deep layers of the common envelope as a significant fraction of the orbital energy is lost during this phase.

- There is strong evidence for significant spin up of gas surrounding the region containing the core of the giant progenitor and the inspiralling companion, reducing the effective gravity and making mass ejection easier.
- Matter is ejected from the common envelope in all directions, with a preference for the orbital plane of the binary system, producing a density contrast in the ejecta between the equatorial and polar directions.
- The efficiency of the mass ejection process, as measured by the ratio of the binding energy of the envelope with respect to the binary system to the orbital energy released from the binary during the common envelope phase, is less than about 40-50%.
- The stabilization of the orbit at small separations during the final phase of the common envelope is easiest for progenitor stars which have steep density gradients above the nuclearly evolved core (so that the mass profile is flat) and/or where the mass of the common envelope is comparable to the mass of the inspiralling companion.

Based on these results, one finds that the survival of the remnant binary as a post spiral in system resulting from the successful ejection of the common envelope is favored for systems in which the giant-like progenitor star

is characterized by larger ratios of the core mass to total mass (roughly greater than about 0.2). Thus, formation of cataclysmic variable type systems is expected to be viable for red giant and asymptotic giant star progenitors with core masses greater than about $0.2M_{\odot}$ and $0.6M_{\odot}$ respectively. For more massive stellar progenitors (i.e., for stars more massive than about $12M_{\odot}$) relevant to the formation of low mass X-ray binary and intermediate mass X-ray binary systems, ejection of the common envelope is favored for advanced evolutionary stages of the progenitor star during its late core helium burning stage and beyond. We note that for stars more massive than about $40M_{\odot}$ stellar winds may significantly affect their evolution, precluding the Roche lobe overflow and mass transfer phase since such stars do not enter the red supergiant phase (32). For systems entering the common envelope phase, significant shrinkage of the binary orbit is possible, leading to a reduction of the orbital separation by more than a factor of 100 from its initial value.

5.2 Ongoing work

Although the calculations that have been carried out in previous studies have provided much insight into the phases of the common envelope stage, calculations at high spatial resolution will be necessary to further quantify the outcome of the common envelope phase. In recent years the development of sophisticated computer methodologies has

made it possible to achieve this goal. Specifically, adaptive mesh refinement techniques have advanced to the point where such calculations can now be envisioned. For a recent review see Norman (33). These methods allow one to maintain high spatial resolution in the core regions as the two cores spiral in together.

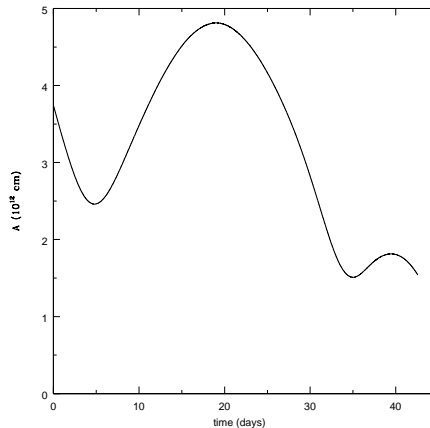


Fig. 9. The orbital separation as a function of time for a system composed of a red giant branch star of $1M_{\odot}$ with a $0.7M_{\odot}$ main sequence companion in which the initial orbital period is 1 month.

Recently, we have initiated high resolution calculations using such techniques. Since the core of the giant and its companion are both too compact to resolve even with an adaptive mesh, and because of their much higher densities with respect to the matter in the common envelope, they couple to the gas primarily via their gravitational fields. Therefore we have modelled the giant core and its companion as particles using an N body solver based on the particle mesh method (34). The companion is represented by a single particle, and the giant core is represented by a uniform, spher-

ical cloud of 2×10^5 particles with core radius three times the smallest zone spacing. All of the particles in the cloud move rigidly together with the cloud’s center of mass. This arrangement ensures that the mapping of particle densities onto the mesh and of the gravitational forces onto the cloud’s center of mass are free of Cartesian grid effects introduced by the use of a cloud-in-cell mapping kernel. An adaptive multigrid solver is used to solve the Poisson equation for the gravitational potential (35; 36). Multigrid algorithms accelerate the convergence of relaxation methods by covering the computational domain with a hierarchy of meshes with different spacings and applying relaxation to each mesh. The single-mesh convergence rate is controlled by error modes having the longest wavelengths compared with the mesh spacing. Thus the longest wavelengths in the domain converge most rapidly on a very coarse mesh. By combining results from all meshes a multigrid algorithm brings all wavelengths into convergence at the same rate.

The use of the adaptive mesh refinement technique and the multigrid method for the gravitational potentials improves on our previous studies (28; 29), allowing calculations not limited to systems of extreme mass ratio, in which the center of mass moves only slightly during the evolution. We have performed several preliminary calculations of the common envelope phase using these techniques in the FLASH code (37). FLASH is an adaptive, parallel, multi-dimensional hydrodynamical

simulation code in which the equations of compressible gas dynamics are solved using the Piecewise-Parabolic Method (38) on a structured, rectangular grid. PPM was developed to provide very accurate solutions for flows containing sharp discontinuities, and it greatly improves upon the hydrodynamics solver used in the nested grid simulations.

As an example, we illustrate the common envelope evolution of a binary system consisting of a $1M_{\odot}$ red giant progenitor with a $0.7M_{\odot}$ main sequence companion at an evolutionary phase when the dynamical evolution occurs on a timescale of about 1 month. The orbital separation of the two cores within the common envelope binary system is illustrated as a function of time in Figure 9. For the case in which the red giant was rotating at half the synchronous rate, the orbit rapidly decayed by a factor of 2 within about 1 month, with the relative orbit passing through two phases of apastron and periastron passage.

In Figure 10, we show the early phases of the spiral in process calculated using FLASH at three time slices at the onset of the evolution (upper 3 panels) and toward the end of the calculation (lower 3 panels) in the innermost 5×10^{12} cm of the binary. The evolution is similar to that described in Section 3, with the development of spiral shock waves emanating from the two cores. However, most importantly, it is seen that the adaptive mesh refinement technique performs very well in resolving the vicinity of the red giant core and the outer layers of the common envelope.

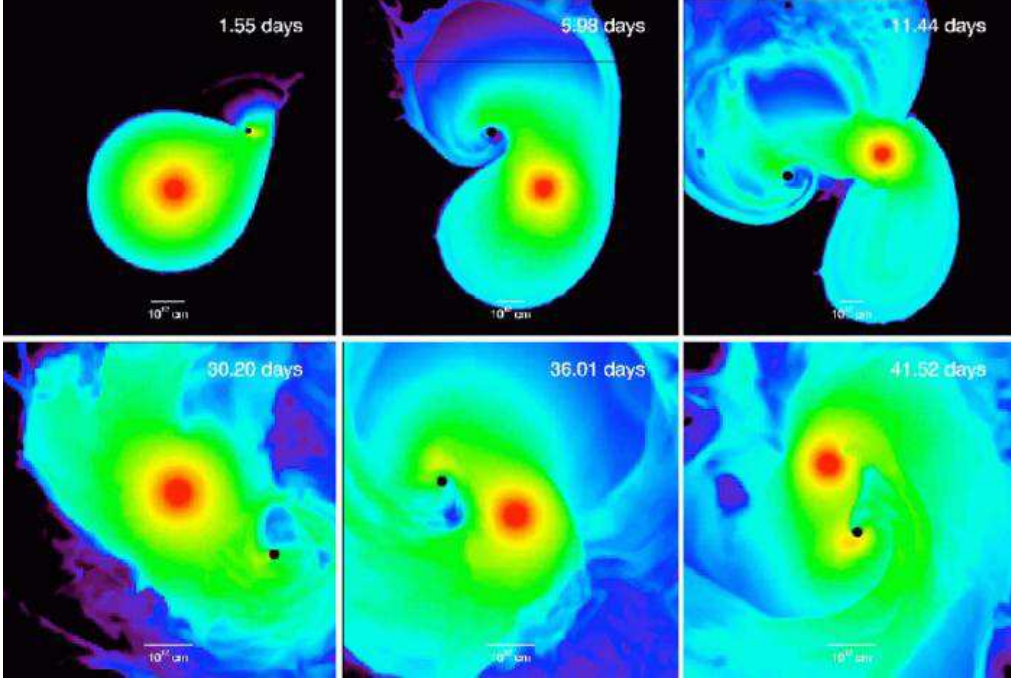


Fig. 10. The density distribution in the orbital plane during the initial and spiral in phase of a binary system composed of a red giant branch star of $1M_{\odot}$ with a $0.7M_{\odot}$ main sequence companion for a system with an initial orbital period of 1 month. Each of the six panels provides the evolution time, which ranges from 1.55 days to 41.52 days. For convenience, a scale of 10^{12} cm is also indicated. The black dot indicates the position of the red giant companion.

We remark that such an evolution could not have been simulated using our previous stationary nested grid technique due to the limitations on the mass of the companion star which, for sufficiently large masses, caused the core of the red giant to move significantly off the highest spatially resolved grid.

Evolutionary calculations such as these in which the innermost regions of the common envelope surrounding the two cores are highly resolved will be necessary to determine whether the binary orbit stabilizes or continues to shrink. Such investigations are essential for determining the dependence of the efficiency of the mass ejection process on the mass of

each component, their evolutionary stage, and orbital separation. Using our model binary systems we plan to systematically investigate the mass ejection process as a function of these system parameters. This is critically important since the generality of the hydrodynamical results with regard to binary system parameters must be ascertained. As two possible mechanisms have been identified for the emergence of the system from the common envelope phase, an exploration of their different dependencies on the binary system parameters is required before definitive conclusions can be drawn for use in population synthesis calculations. This study will allow us to distinguish the regions in progenitor parameter space

for which the post common envelope systems survive from that in which the systems merge into a single rapidly rotating object. Such results will provide important input for population synthesis modeling, allowing us to determine the birth rates for the formation of compact systems in a variety of galactic environments (metal rich star burst regions vs. metal poor regions). The comparison of such rates with observations will allow us to establish the evolutionary channels for these celestial sources.

Acknowledgements

This work was partially supported by the National Center for Supercomputing Applications under grant AST040024 and utilized the NCSA Xeon Linux Cluster. Partial support has also been provided by the NSF through grant AST-0200876. The software used in the FLASH code was developed by the DOE-supported ASC/Alliance Center for Astrophysical Thermonuclear Flashes at the University of Chicago.

References

- [1] E. P. J. van den Heuvel, J. Heise, *Nature Phys. Sci.* **239** (1972) 67.
- [2] F. Verbunt, E. P. J. van den Heuvel, *X-ray Binaries*, W. H. G. Lewin, J. van Paradijs, E. P. J. van den Heuvel, eds. Cambridge University Press, Cambridge, 1995, 457.
- [3] T. M. Tauris, E. van den Heuvel, *Compact Stellar Sources*, W. H. G. Lewin, M. van der Klis, eds. Cambridge University Press, Cambridge, 2005, in press.
- [4] B. Paczynski, *The Structure and Evolution of Close Binary Systems, IAU Symposium No. 73*, P. Eggleton, S. Mitton, J. Whelan, eds. Reidel, Dordrecht, 1976, p. 75.
- [5] I. Iben Jr., M. Livio, *Publ. Astron. Soc. Pac.* **105** (1993) 1373.
- [6] R. E. Taam, E. L. Sandquist, *Annu. Rev. Astron. Astrophys.* **38** (2000) 113.
- [7] C. D. Bailyn, *Nature* **332** (1988) 330.
- [8] F. Rasio, S. L. Shapiro, *Astrophys. J.* **377** (1991) 559.
- [9] S. Sigurdsson, L. Hernquist, *Astrophys. J.* **401** (1992) L93.
- [10] G. H. Darwin, *Proc. R. Soc.* **29**, (1879) 168.
- [11] Z. Kopal, *Astrophys. Space Sci.* **16**, (1972) 3.
- [12] C. C. Counselman, *Astrophys. J.* bf 180, (1973) 307.
- [13] W. M. Sparks, T. P. Stecher, *Astrophys. J.* **188** (1974) 149.
- [14] P. Hut, *Astron. Astrophys.* **92**, (1980) 167.
- [15] M. S. Hjellming, *Ph.D. Thesis*, 1989, University of Illinois.
- [16] A. R. King, M. C. Begelman, *Astrophys. J.* **519** (1999) L127.
- [17] R. E. Taam, P. Bodenheimer, J. P. Ostriker, *Astrophys. J.* **222** (1978) 269.
- [18] F. Meyer, E. Meyer-Hofmeister, *Astron. Astrophys.* **78** (1979) 167.
- [19] A. J. Delgado, *Astron. Astro-*

- phys.* **87** (1980) 343.
- [20] P. Bodenheimer, R. E. Taam, *Astrophys. J.* **280** (1984) 771.
- [21] R. E. Taam, P. Bodenheimer, *Astrophys. J.* **337** (1989) 849.
- [22] R. E. Taam, P. Bodenheimer, *Astrophys. J.* **373** (1991) 246.
- [23] R. E. Taam, P. Bodenheimer, M. Rozyczka, *Astrophys. J.* **431** (1994) 247.
- [24] M. Livio, N. Soker, *Astrophys. J.* **329** (1988) 764.
- [25] J. L. Terman, R. E. Taam, L. Hernquist, *Astrophys. J.* **445** (1995) 367.
- [26] J. L. Terman, R. E. Taam, *Astrophys. J.* **458** (1996) 692.
- [27] F. A. Rasio, M. Livio, *Astrophys. J.* **470** (1996) 1187
- [28] E. L. Sandquist, R. E. Taam, X. Chen, P. Bodenheimer, A. Burkert, *Astrophys. J.* **500** (1998) 909.
- [29] E. L. Sandquist, R. E. Taam, A. Burkert, *Astrophys. J.* **533** (2000) 984.
- [30] G. Nelemans, C. A. Tout, *Monthly Not. R. Astron. Soc.* **356** (2005) 753.
- [31] B. W. Bopp, R. E. Stencel, *Astrophys. J.* **247** (1981) L131.
- [32] D. Vanbeveren, C. DeLoore, W. Van Rensbergen, *Astron. Astrophys. Rev.* **9** (1998), 63.
- [33] M. L. Norman, *Adaptive Mesh Refinement - Theory and Applications*, T. Linde, V. G. Weirs, eds. Springer Verlag, NY, 2005
- [34] R. W. Hockney, J. W. Eastwood, *Computer Simulation Using Particles* (1988)
- [35] A. Brandt, *Math. Comp.* **31** (1977) 333.
- [36] D. Martin, K. Cartwright, *Tech. Rep. UCB/ERK M96/66* (1996).
- [37] B. Fryxell, et al., *Astrophys. J. Suppl.* **131** (2000) 273.
- [38] P. Colella, P. Woodward, *J. Comp. Phys.* **54** (1984) 174.